Hyperdimensional Learning System with Brain-Like Neural Adaptation

ABSTRACT

In the Internet of Things (IoT) domain, many applications are running machine learning algorithms to assimilate the data collected in the swarm of devices. Sending all data to the powerful computing environment, e.g., cloud, poses significant scalability issues coupled with privacy and security concerns. A promising way is to distribute the learning tasks onto the IoT hierarchy; however, the existing sophisticated algorithms such as deep learning are often overcomplex to run on less-powerful IoT devices.

Hyperdimensional Computing (HDC) is a brain-inspired learning approach for efficient and robust learning on today's embedded devices. Encoding, or transforming the input data into high-dimensional representation, is the key first step of HDC before performing a learning task. All existing HDC approaches use a static encoder; thus, they require very high dimensionality, resulting in scalability and efficiency issues. In this paper, we have developed RegenHD, a new HDC approach with a dynamic encoder for adaptive learning. Inspired by human neural regeneration, RegenHD identifies insignificant dimensions and regenerate those dimensions to enhance the learning capability. We also present a scalable learning framework to distribute RegenHD computation over edge devices in IoT systems. Our solution enables edge devices capable of real-time learning from both labeled and unlabeled data. Our evaluation on a wide range of practical classification tasks shows that RegenHD provides 5.7× and 6.1× (12.3× and 14.1×) faster and more energy-efficient training as compared to the HD-based algorithms (DNNs) running on the same platform. RegenHD also provides 4.2× and 11.6× higher robustness to noise in the network and hardware as compared to DNNs.

1. INTRODUCTION

With the emergence of the Internet of Things (IoT), many applications run machine learning algorithms to perform learning and cognitive tasks. Today's systems rely on sending all the data to the cloud, which leads to a significant communication cost [1, 2]. This communication cost can be eliminated by scaling the learning tasks in a distributed fashion where the data are collected from different devices. A mainstream of the research is *federated learning* [1, 3, 4, 5] that trains a central model over multiple devices. However, these techniques use complex algorithms, e.g., Deep Neural Network (DNNs), which require billions of parameters and many hours to train [6, 7]. Considering the memory and resource limitations of the edge devices, IoT systems are still far from real-time learning.

In contrast, the human brain can do much of this learning effortlessly [8,9]. To achieve real-time performance with high energy efficiency, we need to redesign the way of computing that closely models the human brain. HyperDimensional Computing (HDC) mimics important brain functionalities by encoding objects into high dimensional space [9, 10]. HDC is motivated by the observation that the human brain operates on high dimensional representations of data, called *hypervectors*, which have 10,000 or more elements [10]. Because of their high-dimensionality, any randomly chosen pair of hypervectors are nearly orthogonal. HDC is well suited to address learning tasks for IoT systems as: (i) HDC models are computationally efficient to train, highly parallel at heart, and amenable to hardware level optimization [11, 12], (ii) HDC model offers an intuitive and human-interpretable model [13], (iii) it offers a complete computational paradigm that can be applied to cognitive as well as learning problems [8, 13, 14, 15, 16, 17, 18, 19, 20], and (iv) it provides strong robustness to noise [11, 21] – a key strength for IoT systems, and (v) HD can naturally enable secure and lightweight learning [22]. These features make HDC a promising solution for today's embedded devices with limited storage, battery, and resources, as well as future computing systems in deep nano-scaled technology, which devices will have high noise and variability.

Encoding, or transforming the input data into high dimensional representation, is the key first step that leverages randomly generated hypervectors [20, 22, 23]. Mathematically, HDC requires huge dimensionality to provide acceptable accuracy on complex learning tasks. However, increasing dimensionality results in significant efficiency and scalability issues: (i) In high-dimension, HDC involves a large amount of computation, resulting in a significant drop in learning efficiency. (ii) In a distributed system, dimensionality increases data size and communication costs, which are the dominant portion of system efficiency [22]. We observe that the main reason that HDC requires high dimensionality is the encoding module's weakness to find a good representation of the data. During learning, all dimensions of encoded data do not have the same impact on the learning. Many dimensions are insignificant and can drop or replace with no impact on the learning quality. Unfortunately, the existing HD algorithms are using a static encoder with no capability of detecting the importance of dimensions [13, 15, 22, 23]. This is the main reason that HDC algorithms require massive dimensionality to capture all possible relations between the input features.

As a human memory model, HDC needs to use a dynamic and adaptive encoder to map data into high-dimensional space. As shown by several research in neuroscience [24, 25, 26, 27], the neurons in the human brains are dynamically changing. Every day thousands of neurons (brain cells) die and replace by new ones to give a more useful functionality to the brain [28, 29]. In this paper, we proposed RegenHD, a novel adaptive Hyperdimensional learning system. During learning, RegenHD identifies insignificant dimensions and regenerate those dimensions to enhance learning capability. In contrast to the existing methods which use the static encoder to map each input feature into the hyperspace, the proposed solution dynamically regenerates dimensions and explicitly considers non-linear interactions between the inputs. The main contributions of the paper are listed below:

- To the best of our knowledge, **RegenHD is the first HDC algorithm with dynamic and regenerative encoding mod-**

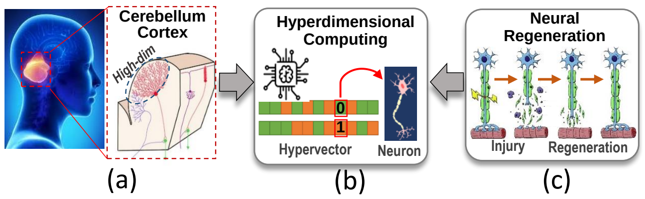

Figure 1: Hyperdimensional computing: model of brain cerebellum cortex

ule. RegenHD identifies insignificant dimensions in an unsupervised way and regenerates them in order to enable dimensions to have a more positive impact on the learning process. RegenHD ensures the learning task performs in a very high effective dimensionality while keeping the physical dimensionality significantly smaller.

- **RegenHD introduces two learning approaches to support dimension regeneration**: (i) *Reset learning* that trains a new model after every regeneration phase, (ii) *Continuous learning* that exploits prior knowledge during the model training. Although *reset learning* is designed for high accuracy, *continuous learning*, inspired by human neural adaptation, provides fast and affordable learning, which is desirable for embedded devices.
- **We present a scalable learning framework to distribute RegenHD computation over edge devices.** We proposed a single-pass training approach that makes edge devices capable of real-time learning from labeled and unlabeled data. Our solution significantly reduces the amount of data communication between edge devices and cloud, resulting in high system efficiency.
- **We show the high robustness of RegenHD to noise in hardware and the network.** Since RegenHD encoding spreads the data over a very large hypervector, a substantial number of bits can be corrupted while preserving sufficient information, resulting in high noise robustness.

We evaluate RegenHD on a wide range of practical classification tasks. Our evaluation shows that the proposed approach achieves much better accuracy than the existing HDC algorithm and comparable accuracy as sophisticated learning algorithms such as SVM and DNN. In terms of efficiency, RegenHD significantly reduces the hypervector dimensionality, resulting in high learning efficiency. For example, RegenHD provides, on average, 5.7× and 6.1× (12.3× and 14.1×) faster and more energy-efficient training as compared to the state-of-the-art HDC algorithms (DNNs). RegenHD also provides 4.2× and 11.6× higher robustness to noise in the network and hardware as compared to DNNs.

2. HYPERDIMENSIONAL COMPUTING

The cerebellum cortex is an area in the brain that plays a significant role in cognitive functions (shown in Figure 1a). Cerebellum receives information from most parts of the body and other brain regions of the brain. Then, it integrates this information and sends signals back to the rest of the brain. The cerebellum is responsible for cognitive functions such as short-term memory and decision making [30, 31]. As researchers continue to unlock the mystery of how billions of neurons in the brain interact, it is becoming more apparent that the cerebellum works as human associative memory. This area of the brain stores the information as a pattern of neural activity in a Purkinje cell layer (Figure 1a).

HyperDimensional Computing (HDC) emerged from theoretical neuroscience as a short-term human memory model [9, 10]. HDC is motivated by the understanding that the cerebellum cortex operates on high-dimensional representations of data that originated from the large size of brain circuits (Figure 1b). It thereby models the human memory using points of a high-dimensional space, that is, with hypervectors. As Figure 1b shows, each dimension of hypervector models a neuron functionality at an abstract level. In high-dimensional space, there exist a huge number of nearly orthogonal hypervectors [10, 32]. This enables us to combine such hypervectors using well-defined operations while keeping the information of the two with high probability.

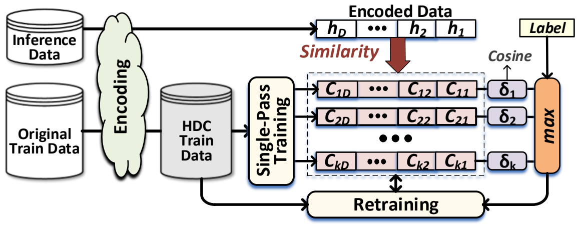

Figure 2: Overview of HD Classification.

2.1 Encoding

Figure 2 shows an overview of the HDC classification task. Regardless of the learning task, the first step of HDC is to encode input data into high-dimensional space, called hypervectors. A hypervector stores all the information across all its components so that no component is more responsible for storing any piece of information than another. HDC uses different encoding methods depending on the data type. The HDC encoding is typically based on a set of primitives: bundling, binding, and permutation. All operations are valid over random vectors in high-dimensional space. Assume $\{\vec{L}_A,\, \vec{L}_B,\, \vec{L}_C,\, \vec{L}_D\}$ as randomly generated hypervectors ($\vec{L}_i \in \{-1,+1\}^D$). These hypervectors are nearly orthogonal, meaning that: $\delta(\vec{L}_A,\, \vec{L}_B) \approx 0$, where δ denotes cosine similarity.
Bundling (+): is defined as an element-wise addition of multiple hypervectors: $H = \vec{L}_A + \vec{L}_B + \vec{L}_C$. The result of bundling is another hypervector with the same dimensionality as inputs. In high-dimensional space, bundling is like a memory operation where the bundled hypervector remembers the input operands' information. For example, we can check the existence of $\vec{L}_A$ and $\vec{L}_R$ on bundled $\vec{H}$ using:

$$\delta(\vec{H},\, \vec{L}_A) >> 0 \qquad \delta(\vec{H},\, \vec{L}_D) \approx 0$$

Binding (∗) : associates the information of multiple objects into a single hypervector. A binding defines as a bitwise `XOR` operation in binary, and multiplication operation in the bipolar domain ($\vec{H} = \vec{L}_A * \vec{L}_B$). The binded hypervector is a new object in high-dimensional space which is orthogonal to all input hypervectors ($\delta(\vec{H},\vec{L}_A) \simeq 0$ and $\delta(\vec{H},\vec{L}_B) \simeq 0$).
permutation (ρ): is defined as a rotational shift operation. A single permutation of a random hypervector generates a new hypervector with nearly orthogonal representation: $\delta(\vec{L}_A,\, \rho\vec{L}_A) \approx 0$. The permutation is suitable for preserving the position of objects in a sequence. In Section 3.3, we describe how HDC encodes different data types using these primitives.

2.2 HDC Learning

Training: after generating each encoding hypervector $\vec{H}^l$

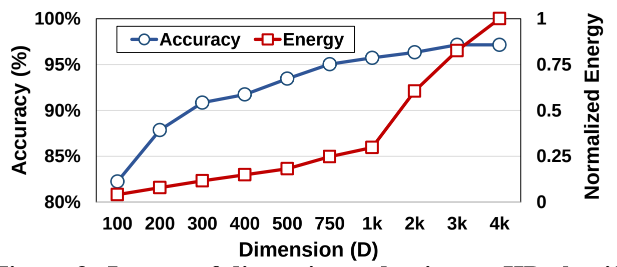

Figure 3: Impact of dimension reduction on HD classification accuracy/efficiency.

of inputs belonging to class/label l, the class hypervector $\vec{C}^l$ can be obtained by bundling (adding) all $\vec{H}^l$s. Assuming there are J inputs having label l: $\vec{C}_l = \sum_j^J \vec{H}_j^l$

Retraining can boost the accuracy of the HD model by discarding the mispredicted queries from corresponding mispredicted classes, and adding them to the right class. Retraining examines if the model correctly returns the label l for an encoded query $\vec{H}$. If the model mispredicts it as label l', the model updates $\vec{C}_l$ and $\vec{C}_{l'}$ as follows:

$$\vec{C}_l = \vec{C}_l + \vec{H} \qquad \& \qquad \vec{C}_{l'} = \vec{C}_{l'} - \vec{H} \tag{1}$$

Inference of HD has a two-step procedure. The first step encodes the input (similar to encoding during training) to produce a query hypervector $\vec{H}$. Thereafter, the similarity (δ) of $\vec{H}$ and all class hypervectors are obtained to find out the class with the highest similarity. Depending on the precision of the hypervectors, RegenHD can use different metrics for similarity search. In binary representation, Hamming distance is a proper similarity metric, while for hypervectors with high precision, cosine distance is used as a similarity metric.

2.3 Challenges

Several research in neuroscience have shown that neurons in the brains are dynamically changing. Every day 85,000 neurons (brain cells) die; that's 31 million in a year [33, 34]. Simultaneously, a similar number of neurons are generating to give more useful functionality to the brain. The generated neurons try to learn new information and help the entire brain system for innovation and adaptive learning. Figure 1c shows brain neural regeneration Hyperdimensional computing, as a brain-inspired computing approach, needs to support a similar behavior. The goal of HDC is to exploit the high-dimensionality of randomly generated base hypervector to represent the information as a pattern of neural activity. Each dimension of the encoded hypervector, in the abstract level, represents a neuron in the brain. Unfortunately, all existing HDC algorithms are using a static encoder. These approaches generate base hypervectors with fixed values and use those bases for the rest of the learning task. All dimensions equally contribute to the learning task. However, in practice, data points and environments are dynamically changing. Thus, they require many dimensions to capture the relation between the input features. However, a large dimensionality has a direct impact on HDC inefficiency. Figure 3 shows the HDC classification accuracy and normalized energy consumption for power prediction in smart home [35]. As the result shows, HDC accuracy and efficiency are both highly dependent on the hypervector dimensionality. Our goal is to design a dynamic HDC encoder that identifies insignificant dimensions and replace them with new dimensions with a more positive impact on the accuracy.

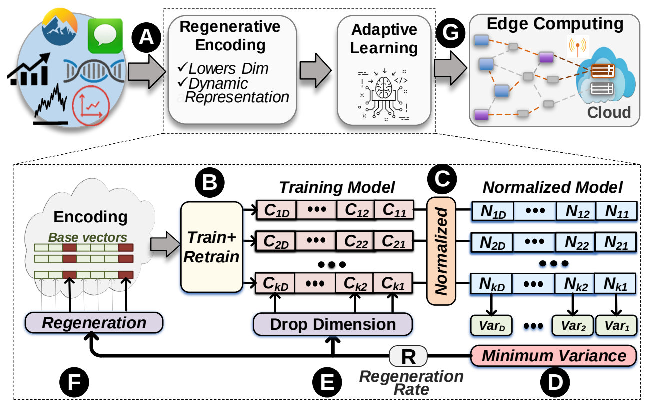

Figure 4: overview of RegenHD using regenerative encoder and adaptive learning.

3. PROPOSED RegenHD

3.1 RegenHD Overview

In this paper, we proposed RegenHD, a novel HDC approach with a dynamic encoder for adaptive learning. In HDC, all dimensions do not have a similar impact on the learning task; There are some dimensions/neurons with no or minimal impact on learning. The goal of our proposed RegenHD is to identify such insignificant dimensions and drop them from the computation. To enhance accuracy, RegenHD extends the model by regenerating those dimensions on the encoding module. This regeneration gives a new chance to dimensions to have a higher contribution to the learning task.

Figure 4 shows an overview of RegenHD learning framework. RegenHD first maps data into high-dimensional space using one of the existing encoding methods (Ⓐ). The encoding depends on the data type and is performed using defined HDC mathematics over a set of randomly generated base vectors (e.g., for text classification as the definition of `A` to `Z` alphabets as random hypervectors in $D = 10k$ dimensions). We explain the details of this static encoder later in Section 3.3. RegenHD performs training over the encoded data (Ⓑ). The trained model is normalized to simplify the similarity metric used in the inference/retraining to dot product operation (Ⓒ) (explained in Section 3.2). Next, we compute the variance over different class dimensions in order to find dimensions with the lowest impact on classification accuracy (Ⓓ). RegenHD drops insignificant dimensions from our model and base hypervectors in the encoder module (Ⓔ)). Finally, RegenHD regenerates the base hypervectors on the selected dimensions (Ⓕ). RegenHD encodes the data points into high-dimensional space using new update base vectors. To continue the learning, RegenHD introduced two iterative learning to repeat training, dimension reduction, and dimension regenerating (explained in Section 3.4). The iterative learning and regeneration continue until RegenHD finds a model that most dimensions are highly contributing to the classification (explained in Section 3.6). We also exploit RegenHD highly compressed and efficient model to enable online learning on edge computing systems (Ⓖ). In the rest of this section, we explain how RegenHD drops and regenerates dimensions, and how iteratively learns to work with new dimensions.

3.2 Drop Insignificant Dimensions

During training, HDC creates a single hypervector representing each class. The inference task happens by checking

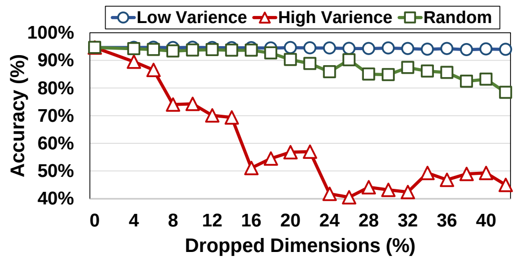

Figure 5: Dropping dimensions and RegenHD classification accuracy.

the similarity of a query hypervector (an encoded inference data) with all class hypervectors. Query data is assigned to a class with the highest similarity. The goal of HDC is to train class hypervectors, where their patterns represent information. A weak classifier cannot find distinct patterns for different classes; thus, many classes will get similar patterns. This makes the classification task hard as the query may have close similarity value to multiple classes.

Figure 2 shows the similarity search of a query, $\vec{H} = \{h_1, h_2, \cdots, h_D\}$, with multiple class hypervectors. During learning, HDC computes the cosine similarity as:

$$\delta(\vec{H}, \vec{C_l}) = \frac{\vec{H} \cdot \vec{C_l}}{\|\vec{H}\| \cdot \|\vec{C_l}\|} = \frac{\vec{H}}{\|\vec{H}\|} \cdot \frac{\vec{C_l}}{\|\vec{C_l}\|} \cong \vec{H} \cdot \vec{N_l} \qquad (2)$$

where $\|\vec{H}\|$ is a repeating factor when comparing a query with all classes, so can be discarded. The $\|\vec{C^l}\|$ factor is also constant for a classes, so only needs to be calculated once. This simplified the cosine similarity to dot product operation.

The same product operation happens between a query and all other classes. As Figure 2 shows, in each dimension, the same query data is multiplied to all class elements on that dimension. Our goal is to find dimensions that do not have a significant impact on the classification task. To this end, as Figure 4D shows, we compute the variance over each dimension of the classes. Dimensions with low variance have similar values over all classes, meaning that they store *common information*. During the search, these dimensions are adding similar weights to cosine over all classes. We call these dimensions insignificant as they do not help to differentiate the class patterns.

RegenHD drops dimensions with low variance (Figure 4E). Figure 5 shows the impact of dimension reduction on RegenHD classification accuracy. In our evaluation, we drop hypervector dimensions in three configurations: (i) dimensions with the lowest variance, (ii) random dimensions, and (iii) dimensions with the highest variance. Our evaluation shows that dropping low variance dimensions has almost no impact on the accuracy while dropping dimensions with higher variance results in significant accuracy drop. Similarly, drooping random dimensions are providing a medium impact on the accuracy drop. This indicates that the low variance dimensions are insignificant and have minimal impact on HDC accuracy.

3.3 RegenHD Dimension Regeneration

RegenHD drops insignificant dimensions and regenerate them during the training phase. Figure 4F shows how this regeneration happens over a dropped dimension. During the training phase, RegenHD creates an initial HDC model, a hypervector representing each class. For each dimension of class hypervector, RegenHD computes the variance over the normalized model (shown in Figure 4D). Then, RegenHD selects $R\%$ of dimensions with minimum variance as a candidate to drop, where R is a regeneration rate. Instead of leaving the drooped dimensions blank, RegenHD re-generates those dimensions. The main goal of regeneration is to create new dimensions that can potentially have a higher impact on the classification, meaning that they can provide a higher variance. Note that RegenHD regeneration is a general approach and applicable to all existing HDC algorithms. In this paper, we look at its impact on the classification task. In the following, we explain the encoding methodology for popular data types and RegenHD modifications during the regeneration phase.

Feature Data: We exploit an encoder method, inspired by the Radial Basis Function (RBF) kernel trick [36, 37], for mapping data points into HD space. This encoder considers the non-linear relation between the features during the encoding. Figure 6a shows our encoding procedure. Let us consider an encoding function that maps a feature vector $\vec{F} = \{f_1, f_2, \ldots, f_n\}$, with n features ($f_i \in \mathbb{R}$) to a hypervector $\vec{H} = \{h_1, h_2, \ldots, h_D\}$ with D dimensions ($h_i \in \{0,1\}$). We generate each dimension of encoded data by calculating a dot product of feature vector with a randomly generated vector as $h_i = cos(\vec{B_i} \cdot \vec{F})$, where B_i is a randomly generated vector from a Gaussian distribution (mean $\mu = 0$ and standard deviation $\sigma = 1$) with the same dimensionality of the feature vector. The random vectors $\{\vec{B}_1, \vec{B}_2, \cdots, \vec{B}_D\}$ can be generated once offline and then can be used for rest of the classification task ($\vec{B_i} \in \mathbb{R}^m$). After this step, each element, h_i of a hypervector $\vec{H}$, represents an encoded dimension.
Regeneration: As Figure 6a shows, each base vector in the encoding module corresponds to generating a single dimension of hypervector. For instance, the i^{th} dimension of encoded data is generated by performing dot product operation between the feature vector and B_i. RegenHD regenerates a selected dimension on the encoding module by updating the corresponding base vector with another randomly generated vector with a Gaussian distribution. The same base update happens on all dimensions that are selected to drop from the class hypervectors.

Text-like Data: The encoding of the text data starts by assigning a random binary hypervector to each character in the alphabet. For example, for encoding the English text, we generate a random hypervector representing digits `A` to `Z` (as shown in Figure 6b). We encode text data in a n-gram windows, where n is usually a number between 3 to 5 [23]. Considering a trigram "`A-B-C`" example, we use the following embedding to map a sequence to high-dimensional space: $\rho\rho\vec{L}_A * \rho\vec{L}_B * \vec{L}_C$. The encoding module binds the hypervectors corresponding to alphabets while exploits permutation to remember their sequence.
regeneration: Due to rotational shift happens by the permutation, the location of dimensions in the base hypervector do not linearly match with the class dimensions on the trained model. Assuming an n-gram windows, a change on the i^{th} dimension of base hypervectors can result in changes on i^{th} to $i+n^{th}$ dimensions of the class hypervectors. Instead of looking for a single dimension of the model with low variance, RegenHD finds the n neighbor dimensions that have the lowest average variance. RegenHD regeneration updates the i^{th} dimension on the base hypervectors, if class dimensions in i^{th} to $(i+n)^{th}$ have minimum average variance. This

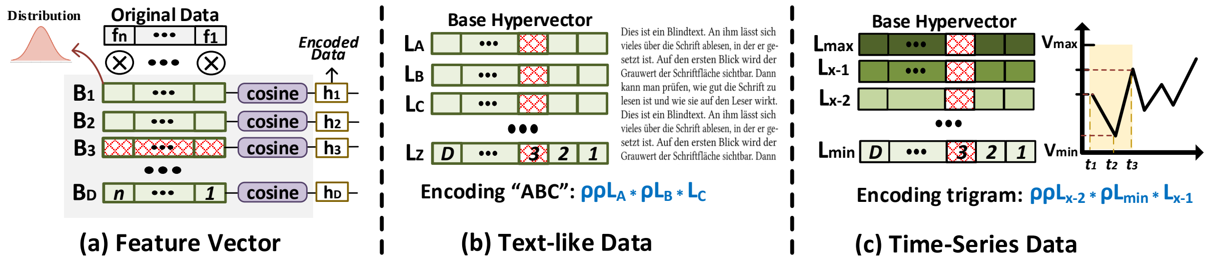

Figure 6: RegenHD encoding and dimension regeneration over different data types.

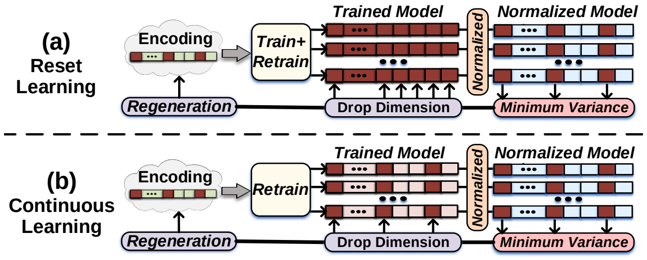

Figure 7: RegenHD reset and continuous learning.

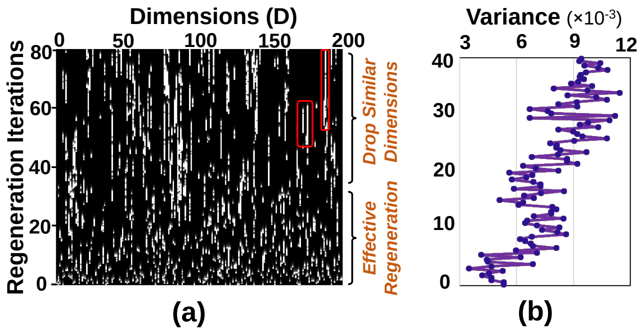

Figure 8: (a) Visualizing the index of regenerated dimensions during different regeneration iterations, (b) Average dimensions variance.

update happens by generating random uniform bits on the i^{th} dimension of all base hypervectors.

Time-Series Data: HDC uses a very similar encoding as text data to map time-series into high-dimensional space. We sample time-series in an n-gram windows. In each sample windows, the signal values (in y-axis) stores the information, and the time (x-axis) represents the sequence. We assign a random vector to V_{min} ($\vec{L}_{min}$ representing minimum signal value) and V_{max} ($\vec{L}_{max}$ representing maximum signal value). Since these vectors are randomly generated, they are nearly orthogonal. For signal values between V_{min} and V_{max}, we perform vector quantization to generate vectors that have a spectrum of similarity to $\vec{L}_{min}$ and $\vec{L}_{max}$ similarity. Finally, the encoding can perform by binding the level hypervectors corresponding to sampled signal, while using permutation to store the timing information. For example shown in Figure 6c, the trigram Windows can be encoded as $\rho\rho\vec{L}_{x-2} * \rho\vec{L}_{min} * \vec{L}_{x-1}$.

Regeneration: Similar to text-data, to select insignificant dimensions, RegenHD computes average variance over n neighbor dimensions of the class hypervectors. Assuming i^{th} to $i+n^{th}$ class dimensions have the minimum average variance, RegenHD drops and regenerates the i^{th} dimension on the $\vec{L}_{min}$ and $\vec{L}_{max}$. The intermediate level hypervectors ($\vec{L}_{x-1}$, and $\vec{L}_{x-2}$ shown in Figure 6C) are computed by performing vector quantization between $\vec{L}_{min}$ and $\vec{L}_{max}$.

3.4 RegenHD Retraining

The regeneration updates the encoding module. However, RegenHD current model still has been trained based on the old bases in the encoding module. To adapt model to count for regeneration, RegenHD proposes two re-training approaches: *Reset Learning* and *Continues Learning*. Reset learning starts training a new model based on the regenerated bases, while *Continues learning* exploits the prior knowledge of the model to continue the learning procedure.

3.4.1 Rest Learning

Figure 15a shows an overview of reset learning. RegenHD starts training a model from scratch using new regenerated bases. This approach does not exploit the information learned by the model in the previous iteration. The training happens by exploiting the new encoded data points and training a hypervector representing each class. Thanks to newly updated base hypervectors, RegenHD is expected to get a larger variance on the regenerated dimensions. This indicates that more number of dimensions are becoming significant and will have a higher impact on the classification. Due to the randomness of the regeneration, it is possible that the newly updated dimension still provides low variance. RegenHD iterative training gives the same change to updated as well as all other dimensions to drop again during the next regeneration iterations. This ensures that RegenHD can find suitable dimensions during the iterative process. Although this approach improves the classification accuracy, it is a slow learning process. Since RegenHD starts each learning iteration from a scratch model (losses the past information), it requires several iterations to converge.

3.4.2 Continuous Learning

Figure 15a shows an overview of continuous learning. RegenHD continues learning from the previously learned model. Instead of start training from scratch, RegenHD only ignores the class values on the dropped dimensions while other dimensions continue learning at the top of their existing values. In each iteration, RegenHD checks the similarity of each training data point with the current model. If the training data point correctly classified with the current model, it does not update the model. However, in the case of miss-classification, RegenHD updates the model by adding the query with correct and subtracting it from the wrong class. This process continues over the entire dataset (or a batch of data) to generate a new model. At the end of the iteration, the new model can be used for the inference task or another iteration of retraining.

3.5 Similarity To Brain Regeneration

RegenHD continuous training has a similar behavior as human neural adaptation, where insignificant neurons die, and newborn neurons perform the same functionality. Like the human brain that evolves more quickly at the young ages (learning phase), RegenHD has more rapid regeneration during the first regeneration iterations. Figure 8a visually shows the index of the regenerated dimensions during different iterations (The white dots show the regenerated dimensions). In the initial regeneration iterations, our approach effectively identifies various dimensions for regeneration. Going further through the regeneration, RegenHD effectively drops insignificant dimensions such that the remaining dimensions are getting a higher and higher variance. Figure 8b shows the average variance of the class hypervector over different dimensions. The results indicate that RegenHD regeneration drops an insignificant dimension and helps find dimensions that can have a higher impact on classification. The increase in the variance depends on the regeneration rate, where higher rates result in a higher increase in the variance.

As Figure 8a shows, the new regenerated dimensions in the last iterations (> 30) will find less chance to compete with already well-developed dimensions in terms of variance. Therefore, RegenHD may repeatedly select the recently regenerated dimensions as the best candidate to drop. Biologically, this is a very similar behavior that neuroscientists observed as the functionality of the human brain [38]. During childhood, the brain regenerates more neurons, while this process slows down by getting aged when the brain gets more complex [34, 39].

3.6 RegenHD Learning Convergence

As we explained, RegenHD is an iterative learning approach that regenerates dimensions through iterations. However, the convergence of RegenHD highly depends on the frequency of the model update and the regeneration rate. Frequently updating the encoding bases can result in model divergence.

Lazy Regeneration: The newly updated dimensions still have very low variance, as these dimensions only retrained for a single iteration. In contrast, other dimensions have been retrained for multiple iterations. During the next regeneration phases, the recently updated dimensions have a higher chance to be selected to drop from the model again. To address this issue, we perform less frequent regeneration, called *lazy regeneration*, rather than updating the encoder in every iteration. This technique ensures that: (i) RegenHD accuracy does not diverge due to aggressive model update, and (ii) regenerated dimensions have enough chance to increase their variance during the iterative learning process. In Section 5.5, we will explore the impact of this lazy regeneration on RegenHD accuracy, stability, and efficiency.

Weighting Dimensions: Another important issue with model regeneration is the small class values on newly generated dimensions. RegenHD training and retraining process increases the values on the class elements. However, the newly updated dimensions usually have small values. During the cosine similarly, the impact of each dimension is determined by its value in each dimension. This means that newly updated dimensions do not have a major impact on the cosine values. To give a similar chance to new dimensions to contribute to the similarity distance, we normalize the class hypervectors over each dimension (shown in Figure 4C). This normalization puts all dimensions values in a similar range as newly generate dimensions. Therefore, all dimensions will have the same chance during the similarity measurement. Note that this normalization happens after every m iterations

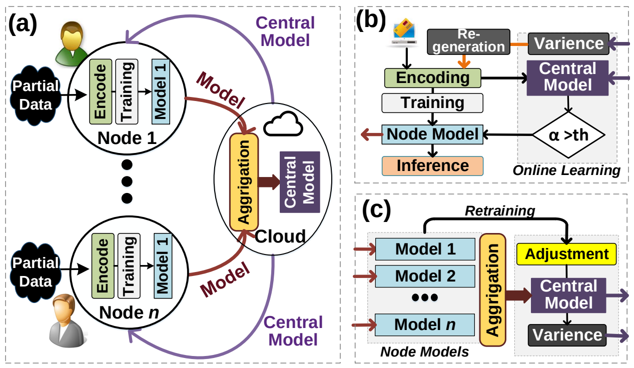

Figure 9: RegenHD federated learning. (a) Overview, (b) Node computation, (c) Cloud computation.

when regeneration happens. During the inference, RegenHD performs the same similarity search as the baseline to find a class with the highest similarity.

4. RegenHD EDGE LEARNING

In IoT systems, devices are connected as a network. A centralized could often receive data from multiple end-node devices, called edge devices. Several research works focused on using neural networks for efficient distributed learning, e.g., federated learning [1, 3, 4, 40]. However, these approaches have the following challenges: (1) Edge devices are often light-weight embedded devices with limited battery, memory, and computing resources. Thus, they cannot provide real-time DNN training, which requires a large memory footprint and computing resources to perform gradient computation. (ii) They suffer from a lack of robustness in both hardware and network noise.

In contrast, RegenHD provides several features that make it suitable for learning in edge learning: (i) fast and real-time learning from the stream of data, and (ii) robustness to noise and failure on the end-node devices and the network. We exploit RegenHD for both centralized and federated learning. In centralized learning, each edge device encodes data into high-dimensional space. All devices send their encoded hypervector to a cloud, and cloud performs learning tasks (learning explained in Section 2.2). The trained model will be shared with all edge devices. Although this approach provides high classification accuracy, it requires a large amount of communication cost, which dominates the total system efficiency. In Section 5.2 and Section 5.3, we evaluate RegenHD accuracy and efficiency in this configuration.

4.1 RegenHD Federated Learning

Figure 9a shows an overview of RegenHD framework supporting federated learning. In federated learning, the encoding and training tasks perform locality on edge devices. Cloud creates an aggregated model by combining models received by all nodes. Then, it shares the aggregated model with all nodes. Each node made necessary changes to the model to personalize it based on its local data. The updated models of all edge devices will be aggregated on the cloud again. This iterative learning continues until generating a central model with the best representation of data received by all nodes. In the following, we explain the details of this iterative learning process.

Edge Learning: Figure 9b shows the functionality of each edge device during federated learning. Each edge device encodes data points into high-dimensional space and trains a local model. RegenHD supports both iterative learning (explained in Section 2.2) or fast single-pass training (explained in Section 4.2). In the first iteration, the learning happens without regenerating the encoding module. RegenHD also supports online learning from both labeled or unlabeled data. The details of learning are explained in Section 4.2.

Cloud Aggregation: Figure 9c shows the functionality of the cloud during federated learning. Cloud receives partially trained models from all edge devices and aggregates them to create a central model. Assume a system with m edge devices, where $\{\vec{C}_i^1, \vec{C}_i^2, \cdots, \vec{C}_i^m\}$ are the i^{th} class hypervectors corresponding to different nodes. RegenHD aggregates the models by adding different patterns corresponding to each node. For example, the i^{th} class of the central model can be created using: $\vec{C}_i^A = \vec{C}_i^1 + \vec{C}_i^2 + \cdots + \vec{C}_i^m$. However, the central model is often saturated by the pattern of dominant nodes, and it does not well represent the entire data. RegenHD addresses this issue by retraining the aggregated model over the class hypervectors received by all nodes. We consider each class hypervector as labeled encoded data. We check the similarity of each class hypervector with the aggregated model. For example, we check the similarity of the i^{th} class hypervector of the node 1 with the aggregated model ($\delta(\vec{C}_i^A, \vec{C}_i^1),\ j \in 1...k$). For every incorrect prediction, RegenHD updates the corresponding class hypervector in the central model as follows:

$$\vec{C}_i^A \leftarrow \vec{C}_i^A + (1 - \delta(\vec{C}_i^A, \vec{C}_i^j)) \times \vec{C}_i^1$$

where '$1 - \delta(\vec{C}_i^A, \vec{C}_i^1)$' term ensures that models do not saturate the class if their pattern already exists in the aggregated model. Cloud continues this retraining in multiple iterations until generating a good representative model.

Cloud Dimension Selection: Cloud performs dimension reduction over the aggregated model, while the regeneration happens locally on each node. Cloud computes the variance on different dimensions of the aggregated model. Then, it sends the central model along with the index of dropped dimensions (variance vector) to all nodes (Figure 9b,c).

Edge Personalized Training: As Figure 9b shows, RegenHD regenerates the base vectors on insignificant dimensions chosen by the cloud. All nodes update the central model locally based on their data points. This is equivalent to personalizing the model in each node. RegenHD supports model adjustment in both iterative or streaming way. In the iterative procedure, each node iterates over the same training data point and updates the model (explained in Section 2.2). RegenHD is also capable of single-pass training where it can update the model based on the stream of data received by each node. We explain the details of RegenHD single-pass training in Section 4.2.

Inference and Continuous Learning: The new model in each node can be used for the inference. To further improve the classification accuracy, RegenHD can continue collaborative learning by aggregating all nodes' models in the cloud. The rest of the learning task repeats as the steps explained above. While RegenHD tries to generate a new aggregated model, edge devices can perform inference based on their most updated model.

4.2 Online Learning on the Edge

One of the main features of HDC is its capability to support single-pass training. RegenHD exploit this feature to enable online learning. In this mode, RegenHD learns a model by one-time passing through each data point, without any iteration. This enables us to perform efficient learning without storing train data. The single-pass training is suitable for many real-world IoT systems where the learning is happening on small embedded devices with limited memory and resources.

Beside supervised learning, RegenHD also supports online learning from semi-supervised data, where only a small portion of training data is labeled. RegenHD first creates a model using labeled data. Then, it exploits unlabeled data to improves the quality of the model. RegenHD checks the similarity of each unlabeled data with the already trained model (Figure 9b). Thanks to RegenHD transparent model, the similarity search gives us confidence about the classification result. The confident level (α) determines how much the model ensures that a data is corresponded to a particulate class. Assume δ_i is a cosine similarity of an encoded data with i^{th} class ($\delta_i = \delta(\vec{H}, \vec{C}_i)$), we compute the confidence of class i^{th} as:

$$\alpha_i = 1 - \frac{\delta_i - \delta_{max \neq i}}{\delta_{max \neq i}}$$

where $\delta_{max \neq i}$ is the class with the maximum similarity to query except with i^{th} class. If the confident level is higher than a threshold (e.g., $\alpha > 90\%$), RegenHD updates the model by embedding encoded data to the corresponding class hypervector as: $\vec{C}^{max} = \vec{C}^{max} + \alpha \times \vec{H}$, where $\vec{H}$ is the query data and $\vec{C}^{max}$ is a class which has the maximum similarity with a query. This approach enables RegenHD to update the model using the stream of unlabeled data.

RegenHD supports regeneration during single-pass training. The dimension reduction used for regeneration is unsupervised, where we can identify insignificant dimensions regardless of the labeled data. During training, RegenHD computes the variance and drops dimensions for the next set of training data points. Then, it regenerates the base vectors in the encoding module to replace insignificant dimensions with more useful ones. RegenHD uses a very low regeneration rate to ensure model convergence. This is because, during the single-pass training, the model does not have a high chance of retraining.

4.3 Robustness to Noise

The technological and fabrication issues in highly scaled technology nodes add a significant amount of noise to both memory and computing units [41,42,43]. Here, we consider the impact of noise on both the edge device and the network. One of the main advantages of RegenHD is its high robustness to noise and failure. In RegenHD, hypervectors are random and holographic with i.i.d. components. Each hypervector stores all the information across all its components so that no component is more responsible for storing any information than another. This makes a hypervector robust against errors in its components. We can exploit RegenHD robustness to optimize total system energy by relaxing the computation as well as communication. In Section 5.7, we explore the robustness of RegenHD to noise in the hardware and the network.

5. EXPERIMENTAL RESULTS

5.1 Experimental Setup

We implement an in-house simulation framework based on NS-3 [44] to evaluate how RegenHD performs on a large-scale distributed learning in IoT. The simulation framework

Table 1: Datasets (n: feature size, K: number of classes)

	n	K	# End Nodes	Train Size	Test Size	Description
MNIST	784	10	NA	60,000	10,000	Handwritten Recognition [47, 48]
ISOLET	617	26	NA	6,238	1,559	Voice Recognition [49]
UCIHAR	561	12	NA	6,213	1,554	Activity Recognition(Mobile) [50]
FACE	608	2	NA	522,441	2,494	Face Recognition [51]
PECAN	312	3	312	22,290	5,574	Urban Electricity Prediction [35]
PAMAP2	75	5	3	611,142	101,582	Activity Recognition(IMU) [52]
APRI	36	2	3	67,017	1,241	Performance Identification [53]
PDP	60	2	5	17,385	7,334	Power Demand Prediction [54]

evaluates RegenHD in a *hardware-in-the-loop* fashion. We use NS-3 to simulate communications on distributed network topologies with diverse network mediums. During the simulation loop, the simulator invokes the RegenHD learning procedures (wrapped with ApplicationContainer of NS-3) on actual platforms that represent different nodes in the IoT hierarchy. We implement RegenHD training and testing on two embedded platforms: FPGA and CPU. For FPGA, we design the RegenHD functionality using Verilog and synthesize it using Xilinx Vivado Design Suite [45]. The synthesis code has been implemented on the Kintex-7 FPGA KC705 Evaluation Kit. We ensure our efficiency is higher than the automated FPGA implementation at [46]. For CPU, the RegenHD code has been written in C++ and optimized for performance. The code has been implemented on Raspberry Pi (RPi) 3B+ using ARM Cortex A53 CPU. For the central node, we developed a CUDA-based implementation of the proposed technique on a server system, which uses Intel Core i7-8700K CPU and NVIDIA GPU GTX 1080 Ti. The simulator collects the execution time and measures power for each connected platform while running the learning procedures. The power consumption are collected by Hioki 3337 power meter.

Table 1 summarizes the evaluated datasets. The tested benchmarks range from relatively small datasets collected in a small IoT network to large data, which includes hundreds of thousands of images of facial and non-facial data. For distributed learning, we use four datasets: (i) **PECAN** presents a dense urban area where a neighborhood may have hundreds of housing units [35]. It has 52 houses observed over the period 2014-01-1 to 2016-12-31. In each house, a set of appliances instrumented with sensors records average energy consumption. The goal is to predict the level of power consumption in the urban area. The prediction results can be used for energy management in smart cities. (ii) **PAMAP2** (Physical activity monitoring) is a dataset for human activity recognition which are widely used to understand user contexts [52]. The data are collected by four sensors (three accelerometers and one heartbeat sensor), producing 75 features in total. (iii) **APRI** (Application performance identification) is collected on a small server cluster which consists of three machines [53]. The server cluster runs Apache Spark applications while collecting performance monitoring counter (PMC) events on each server. The goal is to identify two workload groups depending on their computation intensity. (iv) **PDP** (Power demand prediction) is collected on another high-performance computing cluster consisting of six servers [54]. The goal is to identify either high or low power state of a server using PMC measurements of the other five servers in the cluster. The two datasets for the server systems provide an understanding of efficient task allocations in data centers and microgrids.

5.2 RegenHD Accuracy

RegenHD vs. state-of-the-art: Figure 10a compares the RegenHD accuracy with the state-of-the-art classification algorithms, including Deep Neural Network (DNN), Support Vector Machine (SVM), and AdaBoost. The DNN models are trained with Tensorflow [55], and we exploited the Scikit-learn library [56] for the other algorithms. We exploit the common practice of the grid search to identify the best hyper-parameters for each model. Our evaluation shows that RegenHD provides comparable classification accuracy to the sophisticated non-HDCalgorithms. As compared to the existing HDC algorithms [22, 57], RegenHD can achieve, on average, 9.7% higher classification accuracy, since our new encoding method non-linearly maps data to the high dimensional space whereas the existing HDC algorithms linearly perform the encoding.

RegenHD vs. Baseline: We compare RegenHD accuracy with the state-of-the-art HDC using linear-encoder (Linear-HD). We use RegenHD with static encoder as a baseline that does not have the capability of regeneration (Static-HD). For the Static-HD, results are reported in two dimensionalities: (i) the same physical dimension ($D = 500$) as RegenHD, (ii) the same dimensionality as RegenHD effective dimension (D^*). We define effective dimensionality as the addition of the physical dimensions (D) with the regenerated dimensions through retraining iterations: $D^* = D + R/F \times Iter$, where R, F, and $Iter$ are regeneration rate, regeneration frequency, and the number of iterations, respectively. Our evaluation in Figure 10a shows that RegenHD provides 4.8% higher average accuracy as compared to the Static-HD that uses the same number of physical dimensions. RegenHD accuracy is very comparable to the Static-HD using D^* dimensions. This indicates RegenHD capability in providing high classification accuracy while keeping the physical dimensionality low.

Centralized vs. federated learning: For datasets with multiple users, Figure 10b compares RegenHD accuracy in four configurations: federated and centralized learning using iterative and single-pass training. RegenHD in centralized-iterative learning provides maximum accuracy, as the cloud has access to all train data and can improve accuracy through an iterative learning process. In federated-iterative learning, RegenHD provides very comparable accuracy to the centralized system as each edge device shares its already retrained model with the cloud. Our evaluation shows that federated-iterative learning provides, on average, only 1.1% lower accuracy than RegenHD in centralized-iterative learning. During single-pass training, both centralized and federated learning provide comparable accuracy results, which are slightly lower than RegenHD using iterative approaches. This is because, even in centralized learning, the cloud does not have a chance for iteratively looking at training data points. The lack of retraining in single-pass reduces RegenHD accuracy by 9.4% as compared to iterative learning.

5.3 RegenHD Efficiency

We compare RegenHD efficiency with DNN on two embedded platforms: Raspberry Pi (RPi) 3B+ using ARM CPU and Kintex-7 FPGA. Figure 11a compares RegenHD and the Static-HD efficiency during training and inference phases. The results are normalized to the energy and execution time of DNN running on ARM CPU. Our evaluations show that RegenHD provides higher efficiency than DNN in both training and inference phases. These improvements are higher in the training phase, where RegenHD not only reduces the number of training iterations but also reduces the computation complexity of a single training iteration by eliminating costly gradient computation.

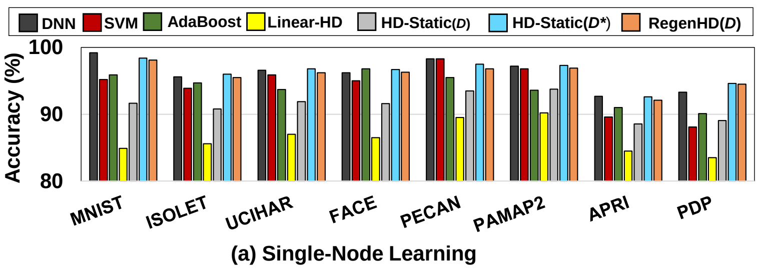

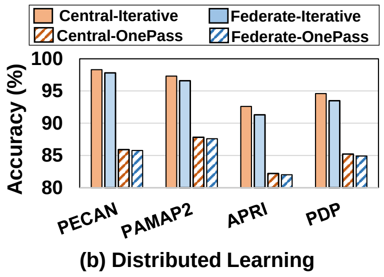

Figure 10: Classification accuracy comparison: (a) learning in a single node, (b) distributed learning

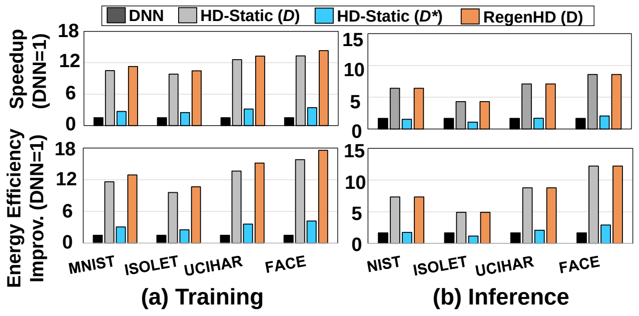

Figure 11: RegenHD training and inference efficiency as compared to Static-HD.

In HDC-based algorithms, i.e., RegenHD and Static-HD, the number of retraining iterations depends on the hypervector dimensionality, where a large dimensionality reduces the number of training iterations. In Static-HD, using D dimensions results in large retraining iterations, where Static-HD using D^* dimensions ($D^* > D$) can be trained with very few iterations. Although the number of RegenHD physical dimensionality is D, its higher effective dimensionality significantly reduces the number of iterations compared to the Static-HD using D dimensions. On the other hand, the efficiency of each training iteration depends on the physical dimensionality. Static-HD with using D dimensional vectors has the highest training efficiency. Although RegenHD has D physical dimensions, the overhead of dimension regeneration increases its single-iteration training cost. The Static-HD with effective dimensionality (D^*) has the lowest single-iteration efficiency, as the training needs to happen over long hypervectors ($D^* > D$). We compute total training efficiency by considering the efficiency-per-iteration along with the number of required iterations. Our evaluation shows that RegenHD provides comparable training efficiency to the Static-HD with D dimensions, while it is 3.6× and 4.2× (12.3× and 14.1×) faster and more energy-efficient than Static-HD with D^* dimensions (DNN).

Figure 11b also compares RegenHD and the baseline HD efficiency during the inference phase. The inference efficiency only depends on the physical dimensionality of the hypervectors. RegenHD and the Static-HD using D physical dimensions provide the same inference efficiency. Our results also indicate that RegenHD is 6.5× faster and 10.5× more energy-efficient than DNN, while providing comparable classification accuracy.

Centralized vs. Federated Learning: We compare the training efficiency of RegenHD using centralized and federated learning. The results are reported in the following configurations: (i) centralized learning where edge devices are CPU (C-CPU) or FPGA (C-FPGA), and (ii) federated learning where edge devices are CPU (F-CPU) or FPGA (F-FPGA). In all configurations, the cloud is a central GPU. We experiment in all configurations when devices are supporting iterative and single-pass training. Figure 12 shows the breakdown of RegenHD computation and communication cost during the training phase. For each application, the results are normalized to C-CPU performing the iterative training. Our evaluation shows that RegenHD in centralized learning relies on a large amount of data movement between end node devices and the cloud. In this configuration, the communication takes a large portion of the training cost, depending on the dimensionality of the encoded data points. Using FPGA as end-node devices has a minor impact on improving RegenHD computational efficiency, as edge devices only perform encoding locality. In this configuration, the major portion of training still performs on the cloud. Since the encoded data in both C-FPGA and C-CPU have the same size, the communication cost remains the same in both configurations.

Federated learning significantly reduces data communication by pushing a significant portion of the training task on the edge devices. Our evaluation shows that RegenHD federated learning (F-CPU) provides on average, 1.6× faster and 1.7× higher energy efficiency than centralized learning (C-CPU). Using FPGA as edge devices result in significant improvement in total efficiency. This is because, in federated learning, edge computation is a large portion of total energy (as shown in Figure 12). For example, our experiments indicate that F-FPGA provides, on average, 1.3× faster and 1.5× energy efficiency as compared to F-CPU.

Figure 12 also compares RegenHD efficiency when cloud and edge devices are supporting single-pass training. During single-pass training, RegenHD significantly improves computation efficiency by eliminating costly iterative training. In centralized learning, this reduction on the computation cost has a minor impact on total RegenHD efficiency, as communication dominates the total RegenHD cost. In contrast, in federated learning, regardless of using CPU or FPGA, the edge computation takes the majority of the training cost. Therefore, single-pass training further reduces the computing cost and makes RegenHD closer to the real-time response. Our evaluation shows that F-FPGA in single-pass learning provides 2.6× and 3.1× (5.4× and 5.8×) faster and higher energy efficiency as compared to F-FPGA (C-FPGA) iterative training.

5.4 RegenHD and Dimensionality

Figure 13 shows the impact of hypervector dimensions on RegenHD and the Static-HD classification accuracy. The Static-HD requires a very large number of dimensions in order to provide high classification accuracy. In contrast, thanks to RegenHD adaptive encoding, our approach provides maximum accuracy in much lower dimensionality. Our evaluations show that reducing the hypervector dimensions from

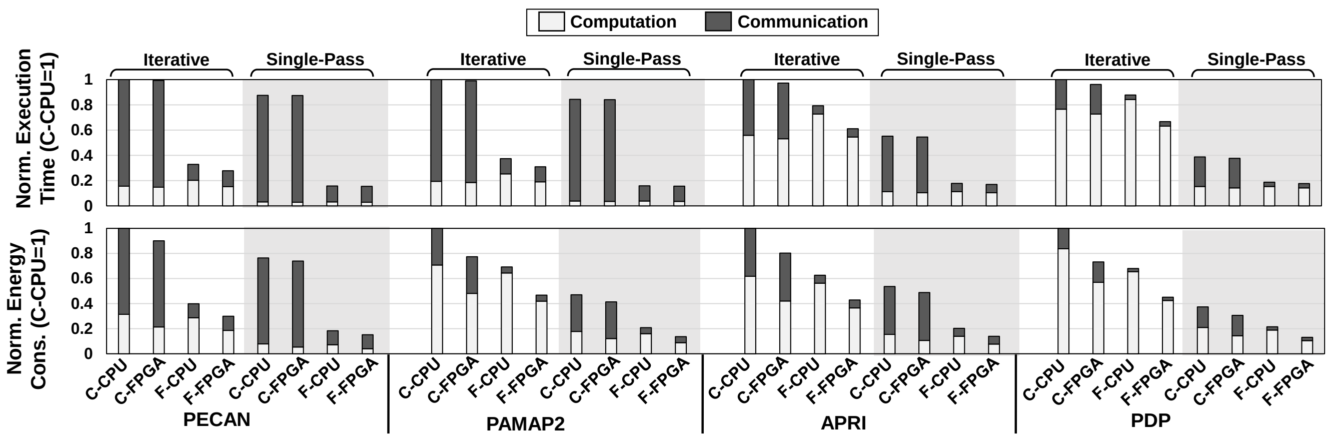

Figure 12: RegenHD efficiency vs state-of-the-art during training and inference.

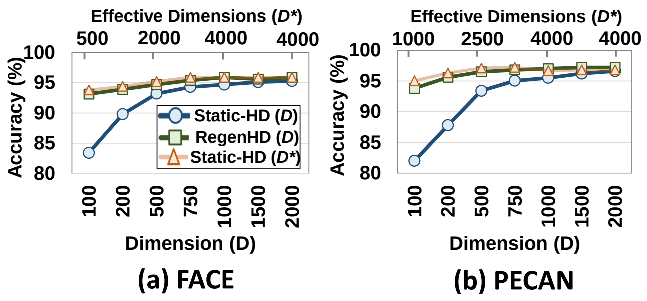

Figure 13: Impact of hypervector dimensions on the accuracy of RegenHD and the Static-HD HD.

$D = 2k$ to $D = 200$, results in 8.5% drop in the Static-HD accuracy. In contrast, RegenHD has much higher robustness to dimension reduction. This is because RegenHD drops insignificant dimensions and replaces them with dimensions that potentially have a higher contribution to the classification. As Figure 13 shows, RegenHD classification accuracy is very comparable to accuracy that Static-HD using the same effective dimensions as RegenHD (shown as an orange line in the figure). Comparing the physical (D) and effective (D^*) dimensions in the bottom and top x-axis of Figure 13, it better indicates RegenHD capability to work with higher dimensions while keeping the number of physical dimensions small.

5.5 Regeneration Rate and Frequency

The rate and frequency of regeneration have a direct impact on RegenHD accuracy and efficiency. Figure 14a shows RegenHD accuracy using different regeneration rates. Our evaluation indicates that using a large regeneration rate or frequency reduces the number of required training iterations. However, this causes significant fluctuation (possible divergence) on the RegenHD accuracy as large regeneration rate drops dimensions, which are not really insignificant (shown in Figure 14a). On the other hand, using a lower regeneration rate and frequency slows down the training process by increasing the required iterations to converge. However, RegenHD will have a smoother change in the accuracy with a lower chance of divergence (shown in Figure 14a).

Figure 14b also shows the impact on regeneration frequency on RegenHD final accuracy. Increasing the frequency of regeneration from $F = 1$ iteration to $F = 5$ iteration results in higher classification accuracy. As discussed in Section 3.6, a large regeneration frequency, i.e., lazy update, gives a higher chance to newly updated dimensions to in-

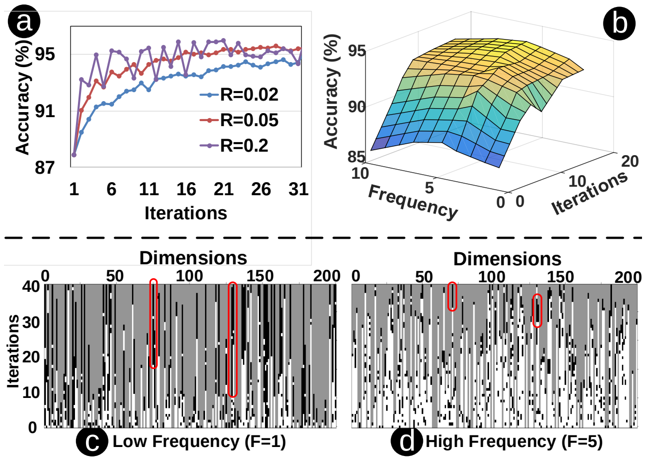

Figure 14: (a)RegenHD accuracy using different regenerated rates (b) RegenHD accuracy using different regeneration frequencies, (c-d) visualizing regenerated dimensions during different regeneration frequencies.

crease their variance through the iterative learning process. Therefore, they would not repeatedly select as candidate dimensions for regeneration. As Figure 14b shows, further increasing the frequency reduces RegenHD effective dimensions resulting in lower classification accuracy. Figure 14b visually shows RegenHD regenerated dimensions (indices) during the learning iterations. As Figure 14a shows, using high regeneration frequency, RegenHD drops and regenerates similar dimensions in every learning iterations. In contrast, using lower frequency, RegenHD regenerates different dimensions through iterations (Figure 14b). In addition, using very large frequency results in less regeneration.

5.6 Reset vs Continuous Learning

We compare RegenHD accuracy and number of iterations using reset and continuous learning (introduced in Section 3.4). The results are reported when both approaches are using the same physical dimension ($D = 500$) and regeneration rate. Our evaluation in Figure 15 shows that RegenHD with reset learning provides higher classification accuracy as compared to continuous learning, while the training takes much longer to converge. The top x-axis in Figure 15 shows the higher accuracy values of reset learning as compared to continuous learning. In Reset learning, RegenHD starts learning a new model in each iteration (from scratch) after

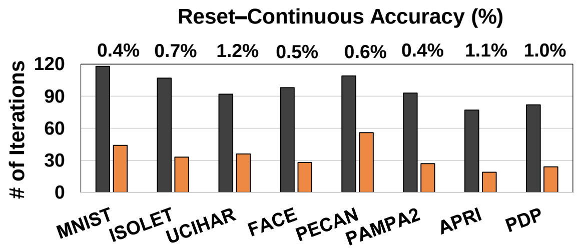

Figure 15: Comparison of reset and continuous learning: accuracy and number of training iterations.

updating the encoding module. In this approach, the loss of prior knowledge slows down the training process. In contrast, continuous learning continues learning from the previously trained model. Although this approach provides faster training, it may result in sub-optimal converges and potentially lower classification accuracy. For learning tasks focused on inference efficiency, Reset learning is a suitable solution as it ensures maximum accuracy. In contrast, for tasks requiring a fast training phase, continuous learning is more suitable as the learning converges with a much lower number of iterations.

5.7 Robustness to Noise

We perform experiments to explore the robustness of RegenHD and DNN to noise in both hardware and network. In RegenHD, information is stored as a holographic distribution of patterns in high-dimensional space. In this representation, all dimensions are equally contributing to store information. Therefore, failures on a packet may only result in failure on a portion of each hypervector, not losing the entire information.

Noise in Hardware: Table 2 reports the average quality loss of DNN and RegenHD during the different percentage of errors in the hardware in edge devices and the cloud. The error rates are the percentage of random bit flips on memory storing neural network and RegenHD models. For fairness, all neural network values quantized to their effective 8-bits representation. In the neural network, random bit flip results in significant quality loss as bit corruptions on most significant bits can cause major changes in the neural network weights. In contrast, RegenHD has higher robustness to noise due to its redundant and holographic distribution. For example, 5% bit flip in hardware results in 16.3% quality loss in the neural network, while this error results in 1.4% (0.9%) quality loss in RegenHD using $D = 500$ ($D = 2k$). RegenHD robustness directly depends on hypervector dimensions. As Table 2 shows, RegenHD in higher dimensionality provides more redundant representation, resulting in higher robustness to noise.

Noise in Network: We explore DNN and RegenHD robustness to noise in the network. The noise is modeled as a loss in random packet during data communication between edge devices and the cloud. Table 2 the quality loss in the classification accuracy for DNN and RegenHD in centralized learning. Our evaluation indicates that DNN has a much higher sensitivity to communication noise as compared to RegenHD. In DNN, losing packets can be equivalent to losing the entire information. In contrast, RegenHD holographic distribution and redundancy increase its robustness to the noise. In centralized learning, edge devices are transferring encoded data points to the cloud. In this configuration, error in the network results in losing a part of encoded hypervector. However, we observe that during the retraining phase, the cloud has a high chance of recovering the lost information by replacing it with other data points with similar patterns.

Table 2: RegenHD quality loss using noisy hardware and the network

Hardware Error	**1%**	**2%**	**5%**	**10%**	**15%**
DNN	3.9%	9.4%	16.3%	26.4%	40.0%
RegenHD ($D = 2k$)	0.0%	0.0%	0.9%	3.1%	5.2%
RegenHD ($D = 0.5k$)	0.0%	0.4%	1.4%	4.7%	7.9%
Network Error	**1%**	**20%**	**40%**	**50%**	**80%**
DNN	0%	2.3%	6.3%	14.5%	37.5%
RegenHD ($D = 2k$)	0%	0.7%	1.3%	3.6%	6.4%
RegenHD ($D = 0.5k$)	0.0%	1.0%	1.9%	5.6%	9.2%

Our evaluations show that adding 40% network noise results in 14.5% quality loss in DNN, while this noise results in less than 3.6% (5.6%) quality loss in RegenHD using $D = 2k$ ($D = 0.5k$) dimensions.

6. RELATED WORK

Edge-Based Learning: Several work studied the feasibility of edge-based learning as a counterpart of the centralized computing [58, 59, 60]. Prior work showed that deep neural networks computation should be split between cloud and edge devices for higher efficiency [5, 61]. These applications rely on neural network applications only limited to inference tasks. Work in [62, 63] rewrote for ML in heterogeneous hierarchical IoT systems, but they are restricted to the linearly decomposable inference computation. Recently, Google also proposed a federated learning approach [40] for collaborative learning. In their approach, each client needs to learn the local model based on the private training data to update the central model in the cloud. Prior work also investigated hot to fuse sensor data streams using ML models [64, 65]. To reduce the amount of transferred data in sensor networks, prior work studied compressive sensing techniques that statistically choose samples and features without losing too much information [66, 67]. These techniques are orthogonal to our method and can be potentially integrated with our learning solution. To summarize, our work is different from the previous work in that it enables distributed learning for both online training and inference tasks.

Hyperdimensional Computing: Since a computational neuroscientist P. Kanerva introduced the field of hyperdimensional computing [9], prior research have applied the idea into diverse cognitive tasks, such as robotics [13, 19], analogy-based reasoning [68], latent semantic analysis [69], language recognition [18], gesture recognition [14], prediction from multimodal sensor fusion [16, 17], and bio-signal processing [70, 71]. For example, the work in [69] proposed a text classification algorithm based on random indexing as a scalable alternative to latent semantic analysis. The work in [14] showed an HDC classification method for biosignal sensory data. Several recent works have presented the hardware accelerator to process the HDC inference task efficiently. For example, work in [11, 21, 72] designed processing in-memory accelerator, which supports all HDC operations inside the memory array. However, all existing HDC algorithms are using a static encoder. This makes these algorithms very inefficient as they require to use large dimensionality to solve realistic problems. In addition, the existing encoding method does not consider non-linear interactions between features, resulting in insufficient prediction accuracy on feature vectors. To the best of our knowledge, RegenHD is the first effort to design an adaptive encoder for HDC. Our approach identifies insignificant dimensions and regenerates them to ensure efficient and scalable learning systems.

7. CONCLUSION

In this paper, we proposed RegenHD, a novel hyperdimensional learning system with a dynamic encoder for adaptive learning. RegenHD identifies dimensions with less impact on the learning task and regenerates them in the encoding module to enhance learning. We show the capability of RegenHD to support online learning from the stream of data received in real-time. Our evaluation shows that RegenHD provides the same accuracy as state-of-the-art HD-based algorithms in much lower physical dimensionality. Therefore, RegenHD provides, on average, $3.6\times$ and $4.2\times$ ($12.3\times$ and $14.1\times$) faster and more energy-efficient training as compared to the HD-based algorithms (DNNs).

8. REFERENCES

[1] X. Wang, Y. Han, C. Wang, Q. Zhao, X. Chen, and M. Chen, "In-edge ai: Intelligentizing mobile edge computing, caching and communication by federated learning," *arXiv preprint arXiv:1809.07857*, 2018.

[2] G. Zhu, D. Liu, Y. Du, C. You, J. Zhang, and K. Huang, "Toward an intelligent edge: wireless communication meets machine learning," *IEEE Communications Magazine*, vol. 58, no. 1, pp. 19–25, 2020.

[3] V. Smith, C.-K. Chiang, M. Sanjabi, and A. S. Talwalkar, "Federated multi-task learning," in *Advances in Neural Information Processing Systems*, pp. 4424–4434, 2017.

[4] E. Bagdasaryan, A. Veit, Y. Hua, D. Estrin, and V. Shmatikov, "How to backdoor federated learning," *arXiv preprint arXiv:1807.00459*, 2018.

[5] Y. Kang, J. Hauswald, C. Gao, A. Rovinski, T. Mudge, J. Mars, and L. Tang, "Neurosurgeon: Collaborative intelligence between the cloud and mobile edge," *ACM SIGPLAN Notices*, vol. 52, no. 4, pp. 615–629, 2017.

[6] J. Pan and J. McElhannon, "Future edge cloud and edge computing for internet of things applications," *IEEE Internet of Things Journal*, vol. 5, no. 1, pp. 439–449, 2017.

[7] H. Li, K. Ota, and M. Dong, "Learning iot in edge: Deep learning for the internet of things with edge computing," *IEEE network*, vol. 32, no. 1, pp. 96–101, 2018.

[8] O. Yilmaz, "Symbolic computation using cellular automata-based hyperdimensional computing," *Neural computation*, vol. 27, no. 12, pp. 2661–2692, 2015.

[9] P. Kanerva, "Hyperdimensional computing: An introduction to computing in distributed representation with high-dimensional random vectors," *Cognitive Computation*, vol. 1, no. 2, pp. 139–159, 2009.

[10] P. Kanerva, J. Kristofersson, and A. Holst, "Random indexing of text samples for latent semantic analysis," in *Proceedings of the 22nd annual conference of the cognitive science society*, vol. 1036, Citeseer, 2000.

[11] M. Imani, A. Rahimi, D. Kong, T. Rosing, and J. M. Rabaey, "Exploring hyperdimensional associative memory," in *High Performance Computer Architecture (HPCA), 2017 IEEE International Symposium on*, pp. 445–456, IEEE, 2017.

[12] T. F. Wu *et al.*, "Brain-inspired computing exploiting carbon nanotube fets and resistive ram: Hyperdimensional computing case study," in *2018 IEEE International Solid-State Circuits Conference-(ISSCC)*, pp. 492–494, IEEE, 2018.

[13] A. Mitrokhin, P. Sutor, C. Fermüller, and Y. Aloimonos, "Learning sensorimotor control with neuromorphic sensors: Toward hyperdimensional active perception," *Science Robotics*, vol. 4, no. 30, p. eaaw6736, 2019.

[14] A. Rahimi, S. Benatti, P. Kanerva, L. Benini, and J. M. Rabaey, "Hyperdimensional biosignal processing: A case study for emg-based hand gesture recognition," in *Rebooting Computing (ICRC), IEEE International Conference on*, pp. 1–8, IEEE, 2016.

[15] A. Mitrokhin, P. Sutor, D. Summers-Stay, C. Fermüller, and Y. Aloimonos, "Symbolic representation and learning with hyperdimensional computing,"

[16] O. Räsänen and S. Kakouros, "Modeling dependencies in multiple parallel data streams with hyperdimensional computing," *IEEE Signal Processing Letters*, vol. 21, no. 7, pp. 899–903, 2014.

[17] O. Rasanen and J. Saarinen, "Sequence prediction with sparse distributed hyperdimensional coding applied to the analysis of mobile phone use patterns," *IEEE Transactions on Neural Networks and Learning Systems*, vol. PP, no. 99, pp. 1–12, 2015.

[18] A. Joshi, J. Halseth, and P. Kanerva, "Language geometry using random indexing," *Quantum Interaction 2016 Conference Proceedings*, In press.

[19] S. Jockel, "Crossmodal learning and prediction of autobiographical episodic experiences using a sparse distributed memory," 2010.

[20] L. Ge and K. K. Parhi, "Classification using hyperdimensional computing: A review," *arXiv preprint arXiv:2004.11204*, 2020.

[21] H. Li, T. F. Wu, A. Rahimi, K.-S. Li, M. Rusch, C.-H. Lin, J.-L. Hsu, M. M. Sabry, S. B. Eryilmaz, J. Sohn, *et al.*, "Hyperdimensional computing with 3d vrram in-memory kernels: Device-architecture co-design for energy-efficient, error-resilient language recognition," in *Electron Devices Meeting (IEDM), 2016 IEEE International*, pp. 16–1, IEEE, 2016.

[22] M. Imani, Y. Kim, S. Riazi, J. Messerly, P. Liu, F. Koushanfar, and T. Rosing, "A framework for collaborative learning in secure high-dimensional space," in *2019 IEEE 12th International Conference on Cloud Computing (CLOUD)*, pp. 435–446, IEEE, 2019.

[23] A. Rahimi, P. Kanerva, and J. M. Rabaey, "A robust and energy-efficient classifier using brain-inspired hyperdimensional computing," in *Proceedings of the 2016 International Symposium on Low Power Electronics and Design*, pp. 64–69, 2016.

[24] J. H. Morrison and P. R. Hof, "Life and death of neurons in the aging brain," *Science*, vol. 278, no. 5337, pp. 412–419, 1997.

[25] E. I. Rugarli and T. Langer, "Mitochondrial quality control: a matter of life and death for neurons," *The EMBO journal*, vol. 31, no. 6, pp. 1336–1349, 2012.

[26] L. Gao, W. Guan, M. Wang, H. Wang, J. Yu, Q. Liu, B. Qiu, Y. Yu, Y. Ping, X. Bian, *et al.*, "Direct generation of human neuronal cells from adult astrocytes by small molecules," *Stem cell reports*, vol. 8, no. 3, pp. 538–547, 2017.

[27] G. Stoll and H. W. Müller, "Nerve injury, axonal degeneration and neural regeneration: basic insights," *Brain pathology*, vol. 9, no. 2, pp. 313–325, 1999.

[28] "Number of new generated neurons every day, nicolas toni." `https://wp.unil.ch/discoverunil/2017/06/we-create-1500-new-neurons-every-day/`.

[29] S. Ackerman *et al.*, *Discovering the brain*. National Academies Press, 1992.

[30] C. J. Stoodley, "The cerebellum and cognition: evidence from functional imaging studies," *The Cerebellum*, vol. 11, no. 2, pp. 352–365, 2012.

[31] P. L. Strick, R. P. Dum, and J. A. Fiez, "Cerebellum and nonmotor function," *Annual review of neuroscience*, vol. 32, pp. 413–434, 2009.

[32] P. Kanerva, "Encoding structure in boolean space," in *ICANN 98*, pp. 387–392, Springer, 1998.

[33] B. Pakkenberg, D. Pelvig, L. Marner, M. J. Bundgaard, H. J. G. Gundersen, J. R. Nyengaard, and L. Regeur, "Aging and the human neocortex," *Experimental gerontology*, vol. 38, no. 1-2, pp. 95–99, 2003.

[34] B. B. Andersen, H. J. G. Gundersen, and B. Pakkenberg, "Aging of the human cerebellum: a stereological study," *Journal of Comparative Neurology*, vol. 466, no. 3, pp. 356–365, 2003.

[35] "Pecan street dataport." `https://dataport.cloud/`.

[36] A. Rahimi and B. Recht, "Random features for large-scale kernel machines," in *Advances in neural information processing systems*, pp. 1177–1184, 2008.

[37] B. Scholkopf, K.-K. Sung, C. J. Burges, F. Girosi, P. Niyogi, T. Poggio, and V. Vapnik, "Comparing support vector machines with gaussian kernels to radial basis function classifiers," *IEEE transactions on Signal Processing*, vol. 45, no. 11, pp. 2758–2765, 1997.

[38] L. Marner, J. R. Nyengaard, Y. Tang, and B. Pakkenberg, "Marked loss of myelinated nerve fibers in the human brain with age," *Journal of comparative neurology*, vol. 462, no. 2, pp. 144–152, 2003.

[39] M. F. Paredes, S. F. Sorrells, A. Cebrian-Silla, K. Sandoval, D. Qi, K. W. Kelley, D. James, S. Mayer, J. Chang, K. I. Auguste, *et al.*, "Does adult neurogenesis persist in the human hippocampus?," *Cell Stem Cell*, vol. 23, no. 6, pp. 780–781, 2018.

[40] K. Bonawitz, V. Ivanov, B. Kreuter, A. Marcedone, H. B. McMahan, S. Patel, D. Ramage, A. Segal, and K. Seth, "Practical secure aggregation for privacy-preserving machine learning," in *Proceedings*

of the 2017 ACM SIGSAC Conference on Computer and Communications Security, pp. 1175–1191, 2017.

[41] S.-H. Lee, "Technology scaling challenges and opportunities of memory devices," in *2016 IEEE International Electron Devices Meeting (IEDM)*, pp. 1–1, IEEE, 2016.

[42] K. T. Lee, W. Kang, E.-A. Chung, G. Kim, H. Shim, H. Lee, H. Kim, M. Choe, N.-I. Lee, A. Patel, *et al.*, "Technology scaling on high-k & metal-gate finfet bti reliability," in *2013 IEEE International Reliability Physics Symposium (IRPS)*, pp. 2D–1, IEEE, 2013.

[43] H. Esmaeilzadeh, E. Blem, R. S. Amant, K. Sankaralingam, and D. Burger, "Dark silicon and the end of multicore scaling," in *Computer Architecture (ISCA), 2011 38th Annual International Symposium on*, pp. 365–376, IEEE, 2011.

[44] T. R. Henderson, M. Lacage, G. F. Riley, C. Dowell, and J. Kopena, "Network simulations with the ns-3 simulator," *SIGCOMM demonstration*, vol. 14, no. 14, p. 527, 2008.

[45] T. Feist, "Vivado design suite," *White Paper*, vol. 5, 2012.

[46] S. Salamat, M. Imani, B. Khaleghi, and T. Rosing, "F5-hd: Fast flexible fpga-based framework for refreshing hyperdimensional computing," in *FPGA*, pp. 53–62, ACM, 2019.

[47] Y. LeCun, L. Bottou, Y. Bengio, and P. Haffner, "Gradient-based learning applied to document recognition," *Proceedings of the IEEE*, vol. 86, no. 11, pp. 2278–2324, 1998.

[48] D. Ciregan, U. Meier, and J. Schmidhuber, "Multi-column deep neural networks for image classification," in *Computer Vision and Pattern Recognition (CVPR), 2012 IEEE Conference on*, pp. 3642–3649, IEEE, 2012.

[49] "Uci machine learning repository." `http://archive.ics.uci.edu/ml/datasets/ISOLET`.

[50] D. Anguita, A. Ghio, L. Oneto, X. Parra, and J. L. Reyes-Ortiz, "Human activity recognition on smartphones using a multiclass hardware-friendly support vector machine," in *International workshop on ambient assisted living*, pp. 216–223, Springer, 2012.

[51] A. Angelova, Y. Abu-Mostafam, and P. Perona, "Pruning training sets for learning of object categories," in *Computer Vision and Pattern Recognition, 2005. CVPR 2005. IEEE Computer Society Conference on*, IEEE, 2005.

[52] A. Reiss and D. Stricker, "Introducing a new benchmarked dataset for activity monitoring," in *Wearable Computers (ISWC), 2012 16th International Symposium on*, pp. 108–109, IEEE, 2012.

[53] M. Zaharia, R. S. Xin, P. Wendell, T. Das, M. Armbrust, A. Dave, X. Meng, J. Rosen, S. Venkataraman, M. J. Franklin, *et al.*, "Apache spark: a unified engine for big data processing," *Communications of the ACM*, vol. 59, no. 11, pp. 56–65, 2016.

[54] Y. Kim, P. Mercati, A. More, E. Shriver, and T. Rosing, "P4: Phase-based power/performance prediction of heterogeneous systems via neural networks," in *Computer-Aided Design (ICCAD), 2017 IEEE/ACM International Conference on*, pp. 683–690, IEEE, 2017.

[55] M. Abadi, A. Agarwal, P. Barham, E. Brevdo, Z. Chen, C. Citro, G. S. Corrado, A. Davis, J. Dean, M. Devin, *et al.*, "Tensorflow: Large-scale machine learning on heterogeneous distributed systems," *arXiv preprint arXiv:1603.04467*, 2016.

[56] F. Pedregosa, G. Varoquaux, A. Gramfort, V. Michel, B. Thirion, O. Grisel, M. Blondel, P. Prettenhofer, R. Weiss, V. Dubourg, *et al.*, "Scikit-learn: Machine learning in python," *Journal of Machine Learning Research*, vol. 12, no. Oct, pp. 2825–2830, 2011.

[57] M. Imani, J. Messerly, F. Wu, W. Pi, and T. Rosing, "A binary learning framework for hyperdimensional computing," in *2019 Design, Automation & Test in Europe Conference & Exhibition (DATE)*, pp. 126–131, IEEE, 2019.

[58] S. Yi, Z. Hao, Z. Qin, and Q. Li, "Fog computing: Platform and applications," in *2015 Third IEEE Workshop on Hot Topics in Web Systems and Technologies (HotWeb)*, pp. 73–78, IEEE, 2015.

[59] L. Tong, Y. Li, and W. Gao, "A hierarchical edge cloud architecture for mobile computing," in *INFOCOM 2016-The 35th Annual IEEE International Conference on Computer Communications, IEEE*, pp. 1–9, IEEE, 2016.

[60] P. Garcia Lopez, A. Montresor, D. Epema, A. Datta, T. Higashino, A. Iamnitchi, M. Barcellos, P. Felber, and E. Riviere, "Edge-centric computing: Vision and challenges," *ACM SIGCOMM Computer Communication Review*, vol. 45, no. 5, pp. 37–42, 2015.

[61] J. H. Ko, T. Na, M. F. Amir, and S. Mukhopadhyay, "Edge-host partitioning of deep neural networks with feature space encoding for resource-constrained internet-of-things platforms," *arXiv preprint arXiv:1802.03835*, 2018.

[62] J. Venkatesh, C. Chan, A. S. Akyurek, and T. S. Rosing, "A modular approach to context-aware iot applications," in *Internet-of-Things Design and Implementation (IoTDI), 2016 IEEE First International Conference on*, pp. 235–240, IEEE, 2016.

[63] H. Grunert and A. Heuer, "Rewriting complex queries from cloud to fog under capability constraints to protect the users' privacy," *Open Journal of Internet Of Things (OJIOT)*, vol. 3, no. 1, pp. 31–45, 2017.

[64] "Aws greengrass." `https://aws.amazon.com/greengrass/`.

[65] B. Khaleghi, A. Khamis, F. O. Karray, and S. N. Razavi, "Multisensor data fusion: A review of the state-of-the-art," *Information fusion*, vol. 14, no. 1, pp. 28–44, 2013.

[66] S. Qaisar, R. M. Bilal, W. Iqbal, M. Naureen, and S. Lee, "Compressive sensing: From theory to applications, a survey," *Journal of Communications and networks*, vol. 15, no. 5, pp. 443–456, 2013.

[67] S. Shalev-Shwartz and S. Ben-David, *Understanding machine learning: From theory to algorithms*. Cambridge university press, 2014.

[68] P. Kanerva, "What we mean when we say "what's the dollar of mexico?": Prototypes and mapping in concept space," in *AAAI Fall Symposium: Quantum Informatics for Cognitive, Social, and Semantic Processes*, pp. 2–6, 2010.

[69] P. Kanerva, J. Kristofersson, and A. Holst, "Random indexing of text samples for latent semantic analysis," in *Proceedings of the 22nd annual conference of the cognitive science society*, vol. 1036, Citeseer, 2000.

[70] A. Burrello, K. Schindler, L. Benini, and A. Rahimi, "One-shot learning for ieeg seizure detection using end-to-end binary operations: Local binary patterns with hyperdimensional computing," in *2018 IEEE Biomedical Circuits and Systems Conference (BioCAS)*, pp. 1–4, IEEE, 2018.

[71] D. Kleyko, A. Rahimi, D. A. Rachkovskij, E. Osipov, and J. M. Rabaey, "Classification and recall with binary hyperdimensional computing: Tradeoffs in choice of density and mapping characteristics," *IEEE transactions on neural networks and learning systems*, no. 99, pp. 1–19, 2018.

[72] T. Wu, P. Huang, A. Rahimi, H. Li, J. Rabaey, P. Wong, and S. Mitra, "Brain-inspired computing exploiting carbon nanotube fets and resistive ram: Hyperdimensional computing case study," in *IEEE Intl. Solid-State Circuits Conference (ISSCC)*, IEEE, 2018.